

Low noise superconducting single photon detectors on silicon

S. N. Dorenbos,^{1,a)} E. M. Reiger,^{1,b)} U. Perinetti,¹ V. Zwiller,¹ T. Zijlstra,² and T. M. Klapwijk²

¹Quantum Transport, Kavli Institute of Nanoscience, TU Delft, 2628CJ Delft, The Netherlands

²Physics of NanoElectronics, Kavli Institute of Nanoscience, TU Delft, 2628CJ Delft, The Netherlands

(Received 8 July 2008; accepted 25 August 2008; published online 29 September 2008)

We have fabricated superconducting nanowire single photon detectors made of NbTiN on a silicon substrate. This type of material reduces the dark count rate by a factor of 10 compared to identical NbN detectors, enabling single photon detection with unprecedented signal to noise ratio: we report a noise equivalent power of 10^{-19} W Hz^{-1/2} at 4.2 K. The compatibility of our superconducting device with silicon enables its integration with complex structures. © 2008 American Institute of Physics. [DOI: 10.1063/1.2990646]

Superconducting single photon detectors (SSPDs) are highly promising detectors because of their high quantum efficiency in the infrared, low jitter, and fast response time.¹ Their working principle is based on the transition from the superconducting to the normal state of a segment of the nanowire under the absorption of a single photon. By a number of characteristics, i.e., high detection rate, SSPDs outperform traditional single photon detectors, such as avalanche photodiodes and photomultiplier tubes, as well as superconducting transition edge sensors² and superconducting tunnel junctions.³ SSPDs were reported in 2001 (Ref. 4) and exhibit single photon sensitivity from the ultraviolet to the mid-IR (up to 6 μm).¹

So far, NbN has been the material of choice for this type of detectors due to the possibility of depositing very thin films (4 nm thick^{5,6}) required for SSPDs. Here, we report on detectors made of NbTiN, a material with critical temperature $T_c=15$ K and critical current density $I_c=5.8 \times 10^6$ A/cm², comparable with NbN ($I_c=2-6 \times 10^6$ A/cm², $T_c=10$ K).⁷ Our NbTiN detectors are fabricated on a silicon substrate, enabling easy integration in advanced electronic circuits. For example, an on-chip amplifier⁸ could overcome problems of impedance matching. Processing the silicon substrate makes integration of an optical cavity and coupling with a fiber⁷ straightforward. We show that a SSPD made of NbTiN gives a lower dark count rate and matches the quantum efficiency of NbN detectors, leading to an improved signal-to-noise ratio.

Figure 1(a) shows a scanning electron microscopy (SEM) image of a NbTiN detector. The detector is a 100 nm wide and about 6 nm thick (based on deposition rate) wire, folded in a $10 \times 10 \mu\text{m}^2$ area. NbTiN thin films were deposited on silicon (with a 225 nm thick oxidized layer) substrates by reactive ion sputtering using a single Nb_{0.7}Ti_{0.3} alloy target in an environment of Ar and N₂ at room temperature. Contacts of 20 nm Nb and 60 nm Au were made using electron beam lithography and lift-off. Subsequently, we defined an etch mask of hydrogen silsesquioxane (HSQ) with electron beam lithography, and the material not covered with HSQ after exposure and development was etched away by reactive ion etching in a plasma of SF₆ and O₂, followed

by the removal of the etch mask with HF. Finally, the samples were glued and bonded on a chip carrier for testing.

The electrical model of the experimental setup is shown in Fig. 1(b). The SSPD is modeled as a switch that opens when a photon is absorbed: a part of the detector becomes resistive ($R_n > 1$ k Ω). The current then flows through the amplifiers, giving a voltage pulse of $V=I_{\text{bias}}R_A A$ (with R_A the amplifier input impedance and A the amplification), provided that $R_n \gg R_A$. Furthermore, the model consists of a kinetic inductance L_k , which limits the counting rate of these detectors.⁹ According to this model, the kinetic inductance relates to the reset time τ as $\tau=L_k/R_A$. The measured reset time is approximately 10 ns, implying a kinetic inductance of 500 nH and a maximum count rate of 100 MHz. The measurements reported here were performed in a liquid helium bath cryostat. An *in situ* microscope objective (0.85 numerical aperture) was used to focus the light on the detector. A tunable laser was used to illuminate the detector with light with a wavelength of 750 and 950 nm and a laser diode was used for light with a wavelength of 650 nm. Scanning the laser spot (1 μm diameter) over the detector (10 μm) revealed a uniform quantum efficiency. The device is biased with a constant current source and voltage pulses are amplified with two amplifiers (total amplification of 46 dB and bandwidth of 10 MHz to 2 GHz) and counted with a pulse counter.

In Fig. 2 the quantum efficiency for different wavelengths is plotted as a function of bias current. All measurements shown in this figure were done on the same device. Each point was measured for 1 s. The quantum efficiency increases exponentially with increasing bias current, as seen

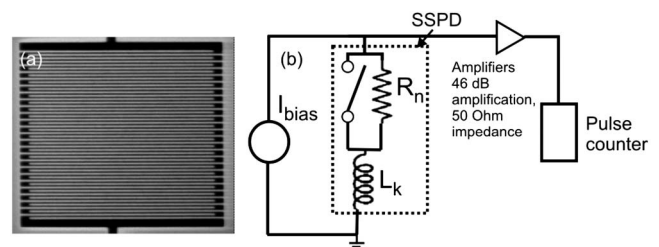


FIG. 1. (a) SEM picture of a NbTiN detector. The detector is $10 \times 10 \mu\text{m}^2$ and the wire is 100 nm wide and 6 nm thick. (b) Electrical model of the SSPD setup. The switch together with the normal resistance $R_n > 1$ k Ω and the kinetic inductance $L_k \approx 500$ nH model the detection principle of the SSPD.

^{a)}Electronic mail: s.n.dorenbos@tudelft.nl.

^{b)}Present address: Institut für Experimentelle und Angewandte Physik, Universität Regensburg, 93040 Regensburg, Germany.

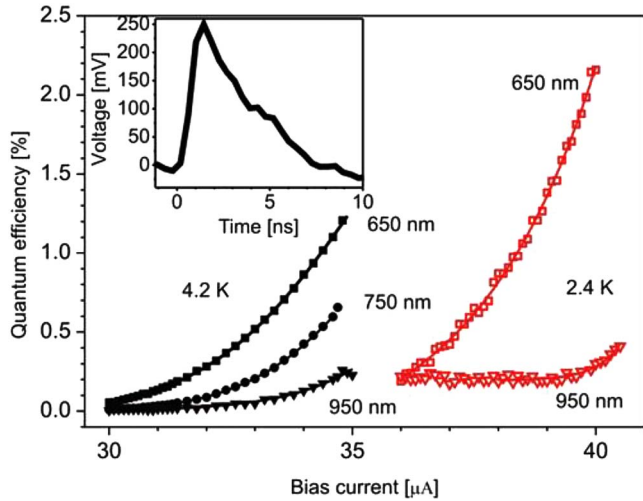


FIG. 2. (Color online) Quantum efficiency vs bias current for different wavelengths and temperatures, with an exponential fit through the data points. Cooling from 4.2 to 2.4 K exhibits an increase in quantum efficiency. In the inset a time trace of a detection event is shown.

from the exponential fit through the data points. The best quantum efficiency is achieved for 650 nm wavelength; for longer wavelengths the efficiency gradually went down. The wavelength dependence of the quantum efficiency can be used to resolve the photon energy.¹⁰ By cooling from 4.2 to 2.4 K, the critical current of the detector increases from 35 μA to 40.5 μA . The quantum efficiency almost doubles, reaching a value as high as 2.3% for 650 nm wavelength. For comparison with literature, we correct for the fill factor (50%) and film absorption (approximately 30%), this corresponds to 14% quantum efficiency. In total, six different devices were measured, with bias currents ranging from 26 to 35.5 μA and calibrated quantum efficiencies ranging from 1.2% to 22.2% at 4.2 K.

In Fig. 3(a) dark counts are shown as a function of bias current and counter trigger level for both a NbTiN (yellow) and a NbN (red) detector. The NbN detector was made from a NbN thin film on a sapphire substrate (commercially obtained⁶), following the same fabrication procedure as the NbTiN detectors. The dark count trace for the NbN detector is comparable to literature.^{1,11} From Fig. 3(a) it can be seen that below a certain counter trigger level (40 mV) the counter mainly detects environmental noise not related to dark counts (detection events without an incident photon) of the superconducting detector. The dark count rate can be measured by raising the trigger level because dark counts have similar voltage pulse amplitudes compared to real detection events (Fig. 2 inset¹²). If the counter trigger level is too high not all photon absorption events are counted, which is not the case for trigger levels of up to 100 mV [Fig. 3(b)]; counter trigger levels of 50–100 mV are optimum for our measurements. The measurement time for the dark count rate [Fig. 3(a)] was 900 s/point between 0.85 I_c and 0.98 I_c and 1 s/point above 0.98 I_c . The lowest dark count rate was $4 \times 10^{-3} \text{ s}^{-1}$. While the quantum efficiency of the NbTiN detectors is as high as for NbN detectors made with the same fabrication procedure, the striking feature of NbTiN detectors is their low dark count rate: a factor of 10 lower compared to NbN detectors. This leads to an unequalled low noise equivalent power (NEP). The NEP is defined to reveal the interplay

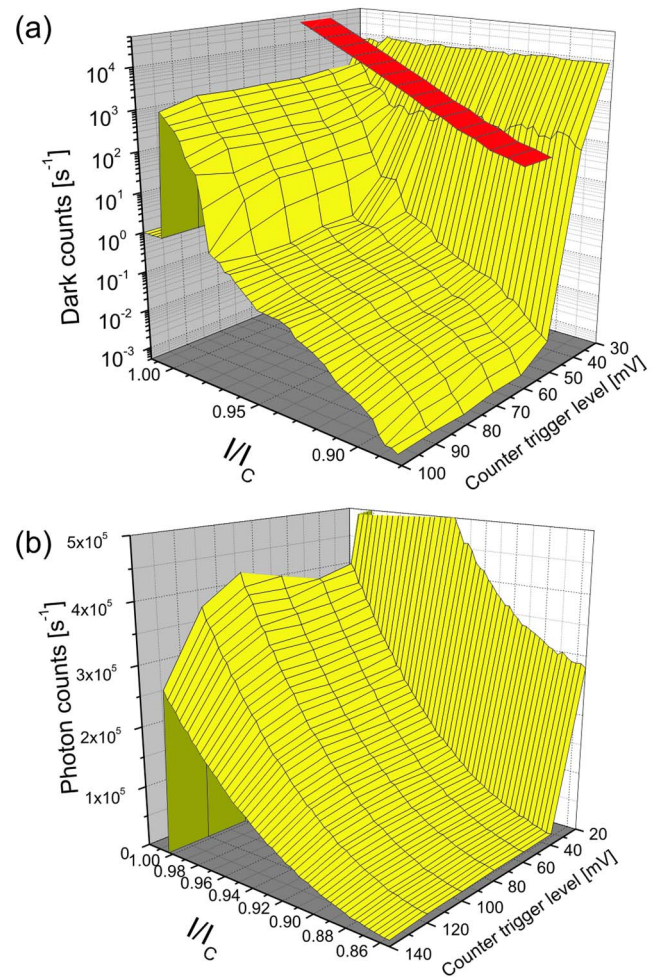


FIG. 3. (Color online) (a) Dark counts as a function of bias current and counter trigger level at a temperature of 4.2 K (yellow). A dark count trace for an identical NbN detector is shown for 60 mV counter trigger level (red). (b) Photon counts/s as a function of bias current and counter trigger level. The incident laser power is 0.01 nW with 650 nm wavelength.

between dark count rate and quantum efficiency,¹³ and is given by

$$\text{NEP} = \frac{h\nu}{\text{QE}} \sqrt{2R_{\text{dc}}}, \quad (1)$$

where $h\nu$ represents the photon energy, QE the quantum efficiency, and R_{dc} the dark count rate. In Fig. 4 the NEP for

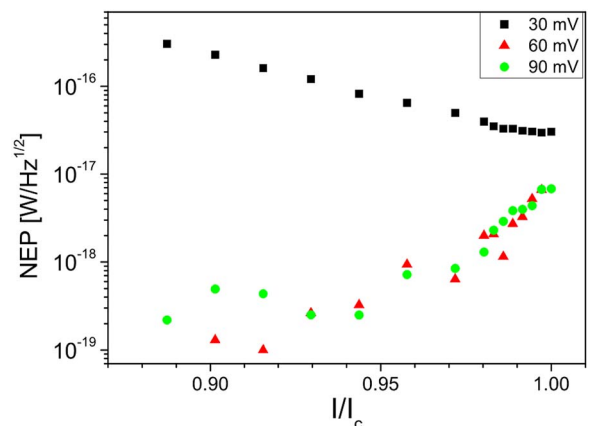


FIG. 4. (Color online) NEP for different trigger levels measured at 4.2 K.

different trigger levels is shown. It can be seen that a NEP of $1 \times 10^{-19} \text{ W Hz}^{-1/2}$ can be reached, two orders of magnitude lower than the best NbN detectors¹¹ and three orders of magnitude lower than typical Si avalanche photodiodes.¹⁴ Note that the NEP reaches $6 \times 10^{-19} \text{ W Hz}^{-1/2}$ very close to the critical current ($0.97I_c$), a desirable behavior, not yet shown for NbN detectors, caused by the fast decrease in dark count rate with decreasing bias current.

We have fabricated SSPDs of NbTiN on a silicon substrate. This type of detectors shows a lower dark count rate compared to NbN detectors processed following the same procedure and measured in the same setup. Presumably, this behavior comes from the fact that a thin layer of NbTiN is less affected by the surroundings than other superconductors.¹⁵ We believe that dark counts are caused by the 2π phase slip of the macroscopic phase,¹⁶ supported by the exponential decrease in dark counts with temperature.¹² Grain boundaries would lead to a reduced free energy barrier (ΔF_0), so we explain the lower dark count rate of NbTiN detectors by a better homogeneity of the superconducting parameters in the NbTiN film compared to NbN. As fabrication on a silicon substrate at room temperature is now possible, integration with advanced structures is within reach.

We acknowledge NWO and FOM for funding. T.Z. and T.M.K. also thank Radionet and Nanoscience-ERA “Nanofridge” for financial support. We thank J. Broeken, O. de Haan, G. Vonk, and J. van der Wolf for their help with the experiment, and L. Kouwenhoven, M. de Dood, R. Sobolewski, and J. Kitaygorsky for discussions.

¹G. Gol'tsman, O. Minaeva, A. Korneev, M. Tarkhov, I. Rubtsova, A. Divochiy, I. Milostnaya, G. Chulkova, N. Kaurova, B. Voronov, D. Pan, J. Kitaygorsky, A. Cross, A. Pearlman, I. Komissarov, W. Slysz, M. Wegrzecki, P. Grabiec, and R. Sobolewski, *IEEE Trans. Appl. Supercond.* **17**, 246 (2007).

²P. Mauskopf, D. Morozov, D. Glowack, D. Goldie, S. Withington, M.

Bruijn, P. DeKorte, H. Hoevers, M. Ridder, J. van der Kuur, and J. Gao, *Proc. SPIE* **7020**, 22 (2008).

³A. Peacock, P. Verhoeve, N. Rando, A. van Dordrecht, B. G. Taylor, C. Erd, M. A. C. Perryman, R. Venn, J. Howlett, D. J. Goldie, J. Lumley, and M. Wallis, *Nature (London)* **381**, 135 (1996).

⁴G. Gol'tsman, O. Okunev, G. Chulkova, A. Lipatov, A. Semenov, K. Smirnov, B. Voronov, A. Dzardanov, C. Williams, and R. Sobolewski, *Appl. Phys. Lett.* **79**, 705 (2001).

⁵J. R. Gao, M. Hajenius, F. D. Tichelaar, T. M. Klapwijk, B. Voronov, E. Grishin, G. Gol'tsman, C. A. Zorman, and M. Mehregany, *Appl. Phys. Lett.* **91**, 062504 (2007).

⁶G. Gol'tsman, K. Smirnov, P. Kouminov, B. Voronov, N. Kaurova, V. Drakinsky, J. Zhang, A. Verevkin, and R. Sobolewski, *IEEE Trans. Appl. Supercond.* **13**, 192 (2003).

⁷W. Slysz, M. Wegrzecki, J. Bar, M. Gorska, V. Zwiller, C. Latta, P. Bohi, I. Milostnaya, O. Minaeva, A. Antipov, O. Okunev, A. Korneev, K. Smirnov, B. Voronov, N. Kaurova, G. Gol'tsman, A. Pearlman, A. Cross, I. Komissarov, A. Verevkin, and R. Sobolewski, *Appl. Phys. Lett.* **88**, 261113 (2006).

⁸J. Kitaygorsky, R. Schouten, S. Dorenbos, E. Reiger, V. Zwiller, and R. Sobolewski, “Measurements of amplitude distributions of dark counts and photon counts in NbN superconducting single-photon detectors integrated with the HEMT read-out,” *J. Mod. Opt.* (submitted).

⁹A. Kerman, E. Dauler, W. Keich, J. Yang, K. Berggren, G. Gol'tsman, and B. Voronov, *Appl. Phys. Lett.* **88**, 111116 (2006).

¹⁰E. Reiger, S. Dorenbos, V. Zwiller, A. Korneev, G. Chulkova, I. Milostnaya, O. Minaeva, G. Gol'tsman, W. Slysz, J. Kitaygorsky, D. Pan, A. Jukna, and R. Sobolewski, *IEEE J. Sel. Top. Quantum Electron.* **13**, 934 (2007).

¹¹A. Korneev, V. Matvienko, O. Minaeva, I. Milostnaya, I. Rubtsova, G. Chulkova, K. Smirnov, V. Voronov, G. Gol'tsman, W. Slysz, A. Pearlman, A. Verevkin, and R. Sobolewski, *IEEE Trans. Appl. Supercond.* **15**, 571 (2005).

¹²J. Kitaygorsky, J. Zhang, A. Verevkin, A. Sergeev, A. Korneev, V. Matvienko, P. Kouminov, K. Smirnov, B. Voronov, G. Gol'tsman, and R. Sobolewski, *IEEE Trans. Appl. Supercond.* **15**, 545 (2005).

¹³G. Rieke, *Detection of Light, from UV to Submillimeter*, 2nd ed. (Cambridge University Press, Cambridge, England, 2002).

¹⁴See optoelectronics.perkinelmer.com for specifications of silicon APDs.

¹⁵R. Barends, H. L. Hortensius, T. Zijlstra, J. J. A. Baselmans, S. J. C. Yates, J. R. Gao, and T. M. Klapwijk, *Appl. Phys. Lett.* **92**, 223502 (2008).

¹⁶M. Tinkham, *Introduction to Superconductivity*, 2nd ed. (Dover, New York, 1996).